Identification of Fog with NOAA AVHRR Images

Jun-ichi Kudoh and Shoichi Noguchi

Abstract—**Fog often occurs from June to September on the Pacific side of northern Japan. As a consequence of poor visibility, there are many disasters at sea. By identifying fog using satellite data, accidents at sea could be reduced. In this paper, we attempted to identify fog using image-processing data from the NOAA Advanced Very High Resolution Radiometer (AVHRR). AVHRR sensors measure radiation at visible, near-infrared, and infrared wavelengths. Here we restrict our attention to daytime data from channel 1 (CH1), channel 3 (CH3), and channel 4 (CH4) for a detection range of $\lambda = 0.58 \sim 0.68$ μm, $\lambda = 3.55 \sim 3.93$ μm, and $\lambda = 10.5 \sim 11.5$ μm, respectively. We define the fog in this paper as observed by a lighthouse keeper. We use CH3 and CH4 because these channels contain the thermal information of such fog. We have analyzed by image processing, the data obtained from CH1, CH3, and CH4, by forming two- and three-dimensional histograms and enhancing them in color. The fog analysis technique enables a nonmeterologist to have a preliminary guess regarding the regions of fog in this histogram.**

I. Introduction

FOG often occurs from June to September on the Pacific side of northern Japan. During this period, as a consequence, there are many disasters at sea. If fog location and area are known, accidents at sea can be reduced. This can be achieved by processing image data from the National Oceanic and Atmospheric Administration (NOAA) [1] satellites that are received every day.

There are sometimes very small differences between fog and other cloud types as detected by satellite. In reality, fog is low-lying cloud that impairs navigators. The Glossary of Meteorology requires visibility in fog to be less than 1 km [2].

In this paper, we explain the term fog in Section II, because the exact meaning of fog should be made clear before defining its detection methodology. From an image processing standpoint [3], we tried to identify the fog using a two- and three-dimensional analysis method. In our suggested fog detection and analysis method, the X, Y, and Z axes of histogram directly correspond to CH1, CH3, and CH4, respectively. The occurred clusters in this spatial distribution are analyzed by comparing land information [4]. This analysis can serve as a preliminary guess for use by a nonmeteorologist.

Manuscript received August 16, 1990; revised April 27, 1991.

J. Kudoh is with the Computer Center, Tohoku University, Japan.

S. Noguchi is with the Research Center for Applied Information Sciences.

IEEE Log Number 9101478.

TABLE I
MEASURED WEATHER CONDITIONS AT SELECTED COASTAL STATIONS ON AUGUST 4, 1989
(Visibility by lighthouse keeper)

Time (JAPAN) 1989.08.04	(A) Shiriya (N:41° 26′) (E:141° 28′)	(B) Ohma (N:41° 33′) (E:140° 55′)	(C) Kinkasan (N:38° 17′) (E:141° 34′)
6:15			Fog(500 m)
6:22		Fog(200 m)	
6:25	Fog(200 m)		
7:06		NOAA-10 Measurement	
7:15			Cloud(1000 m)
7:22		Fog(200 m)	
7:25	Fog(300 m)		

II. Definition of Fog in This Study

We define fog in our study as follows: (1) Season: from June to September; (2) Area: Tohoku area on the Pacific side of northern Japan; and (3) Identification: observation by a lighthouse keeper. Also, as the first step in this paper, we have considered satellite and ground-based observations, during morning time. Therefore, satellite data are limited to NOAA-10, which passes overhead at about 0700 local time each day. In this case, surface observations of fog were supplied by Second Region Maritime Safe Agency Headquarters. Table I lists the part of data by location, observation time, weather conditions, and visibility. In this paper, the term "cloud" means clouds other than fog.

III. Relationship Between Fog and NOAA AVHRR Images

A. NOAA AVHRR Images

The detailed ranges of the multispectral images of NOAA AVHRR [5] are: CH1: ($\lambda = 0.58 \sim 0.68$ μm: visible); CH2: ($\lambda = 0.73 \sim 1.10$ μm: near-infrared); CH3: ($\lambda = 3.55 \sim 3.93$ μm: infrared); CH4: ($\lambda = 10.5 \sim 11.5$ μm: infrared); and CH5: ($\lambda = 11.5 \sim 12.5$ μm: infrared.

The subject location is Tohoku in Japan, situated north of Tokyo. The image area is divided into 1024 × 1024 pixels (1 pixel is nominally 1.1 km) centered on the Tohoku region. The target channel is from CH1 to CH4 because the NOAA-10 AVHRR has no CH5. These channel images are navigated geographically. Especially as a result of calibration, CH4 consist of brightness temperature images. Although one pixel of the original data was 10 b it was normalized to 8 b and all pictures were thinned out

0196-2892/91/0900-0704$01.00 © 1991 IEEE

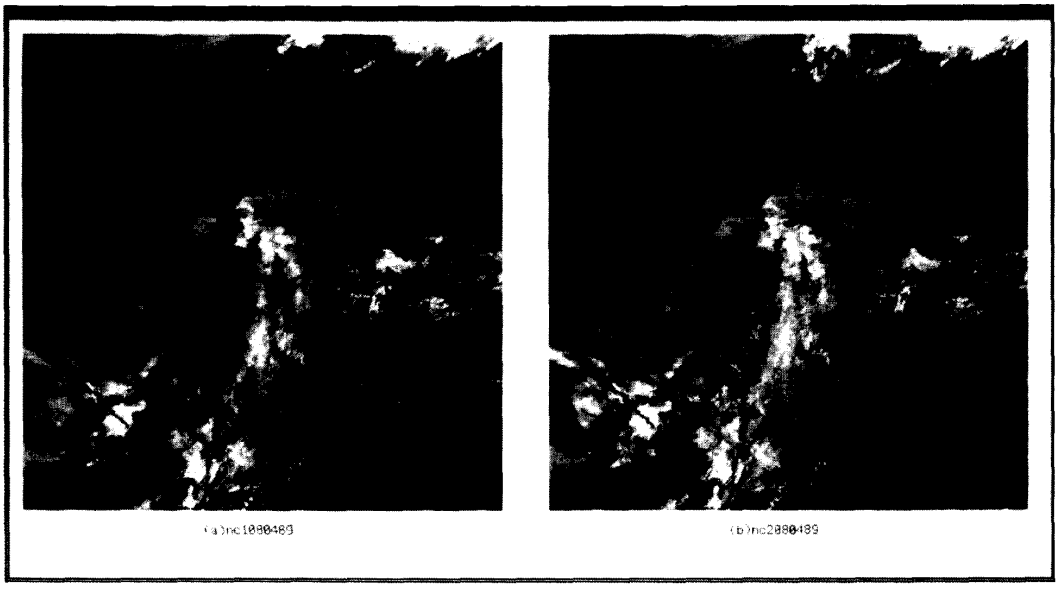

(a) (b)

Fig. 1. NOAA AVHRR images: (a) CH1, (b) CH2.

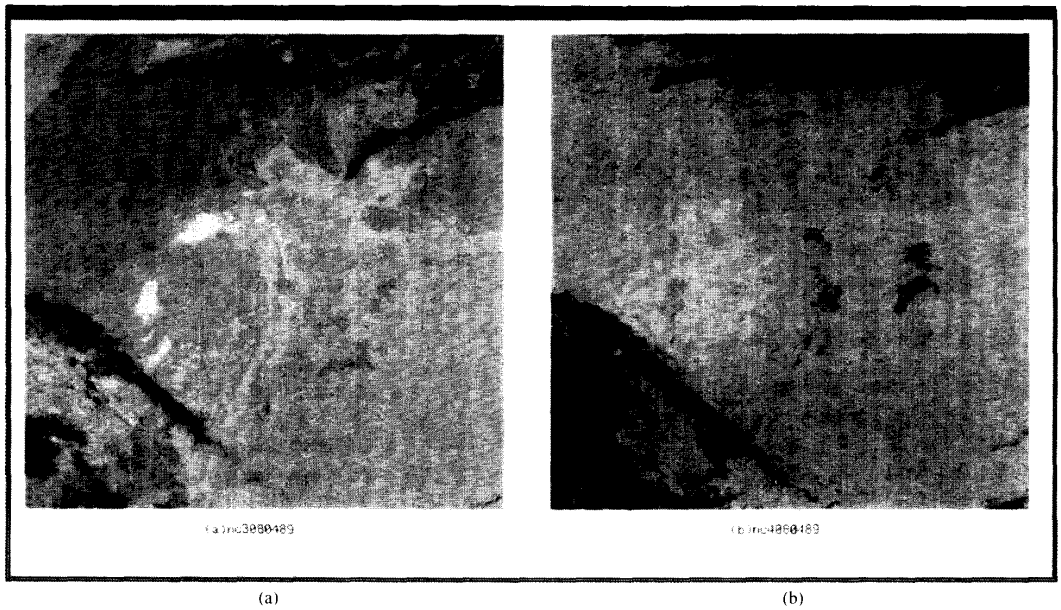

(a) (b)

Fig. 2. NOAA AVHRR images: (a) CH3, (b) CH4.

to 512 × 512 pixels because of memory size limitations and processing time requirements.

B. Observation of Images

CH1 and CH2 subject scenes are shown in Fig. 1(a and b), with the contrast enhanced for display purposes. Fig. 2(a and b) shows the same for a CH3 and CH4 image. We cannot recognize the existence of noise in all these images. The data of these figures were recorded at 0706 local time on August 4, 1989, corresponding to 2206 UTC on August 3, 1989.

Fig. 1(a) is from CH1, in which land areas are difficult to recognize. Fig. 1(b) is from CH2, in which land areas can be recognized clearly. CH1 is more suitable for fog detection than CH2. So, CH1 is used for fog identifica-

tion, thereby reducing the chance of confusing fog with land. Fig. 2 contains infrared images. Fig. 2(a) is from CH3, which is in an infrared atmospheric window. Although it is difficult to use CH3 in daytime because of both emitted thermal and reflected solar contributions to the upwelling radiance [6], [7], we found that it is possible to make use of most of the CH3 data in our two- and three-dimensional analysis. Fig. 2(b) is from CH4, which measures far-infrared thermal radiation. CH4 has been converted to brightness temperatures. High temperatures are white and low temperatures are black in Fig. 2(b).

IV. Histograms and Image Analysis

A. Two-Dimensional Histogram

A two-dimensional histogram technique is a processing method for the two image channels of the NOAA AVHRR to the X, Y axes of a graph whose axes are the brightness or gray-level values between 0 and 255. As this histogram displays the information of the two images at the same time, it is possible to extract feature information or clustering of meteorological objects in the pictures. This is a method that has been applied successfully to general systems [8]–[10].

B. Two-Dimensional Analysis

Fig. 3(b) shows the results of a two-dimensional analysis using CH1 and CH3. In Fig. 3(a), latitude and longitude along with the boundary line of Japan is superimposed on the CH1 image. It can be seen from Table I that fog was detected at Shiriya (N:41° 26′, E:141° 28′) at 0625 and 0725 local time. So, in the pass for NOAA-10 at 0706 local, which is in between the above observation times, the image should contain fog. In Fig. 3(a), the yellow cursor is placed at Shiriya. At this location the image data of CH1 and CH3 ar nc1080489 and nc3080489, respectively, and their values of brightness are 46 and 201. The first digit of image data is the channel number and the rest is observation date (CH#-month-day-year).

Fig. 3(b) is a two-dimensional histogram, the frequency of X, Y values are displayed as gray-levels from black to white. The lowest frequencies were painted in white in order to obtain a clear picture. Fig. 3(a) image information at the location of the yellow cursor is marked by a circle on the histogram in Fig. 3(b).

In this case, the boundary of the cluster belonging to the circle marked is unclear, so it is difficult to identify the cluster exactly. It appears, as a first guess, that the gray area around the circle might be a fog cluster in the two-dimensional histogram.

C. Three-Dimensional Histogram

A three-dimensional histogram technique is a method which displays the brightness values between $0 \sim 255$ of the three images from the three different channels of the NOAA AVHRR to the three X, Y, and Z axes of a graph. This histogram contains the information of each individual image at the same time, so that it is possible to extract property information or clustering of the subject explicitly.

The three images are image1, image2, and image3, corresponding to CH1, CH3, and CH4. The length and breadth of an image is described as x and y. The brightness values of the pixel are I_1, I_2, and I_3, which correspond to three images of image1, image2, and image3, respectively. In this study, three-dimensional spatial distribution means the brightness distribution of I_1, I_2, and I_3. As all the images from CH1 to CH4 have 512×512 pixel and 256 levels, the ranges of (x, y) and $[I_1, I_2, I_3]$ are as follows:

$$(0, 0) \le (x, y) \le (511, 511) \tag{1}$$

$$[0, 0, 0] \le [I_1, I_2, I_3] \le [255, 255, 255] \tag{2}$$

where, ( ) is coordinates of the length and breadth of an image, and where [ ] is the axis of coordinates of the brightness of image1, image2, and image3. In these three images the pixel number P, which is counted by scanning the images, and corresponds to α_1, α_2, and α_3 of the images, is described by (3):

$$P[I_1, I_2, I_3] = \sum_{x=0}^{511} \sum_{y=0}^{511} \delta\{\alpha_1, I_1(x, y)\} \cdot \delta\{\alpha_2, I_2(x, y)\} \cdot \delta\{\alpha_3, I_3(x, y)\} \tag{3}$$

$$[0, 0, 0] \le [\alpha_1, \alpha_2, \alpha_3] \le [255, 255, 255]. \tag{4}$$

The range of P is described by (5):

$$0 \le P \le 512 \times 512 \tag{5}$$

where, $\delta\{i, j\} \equiv \delta_{ij}$ is Kronecker delta [14].

The distributed of P corresponds to the components of the individual images, which depends on the physical properties of three channels. Thus the distribution of P in the three brightness spatial distribution is obtained by scanning all areas of $\alpha_1 \sim \alpha_3$. This distribution is the most important part of fog analysis. For the display method of the three-dimensional histogram of the NOAA AVHRR images, refer to J. Kudoh and S. Noguchi [13].

D. Three-Dimensional Analysis

Fig. 4(b) is a three-dimensional histogram, in which X, Y, and Z axes correspond to CH1, CH4, and CH3, respectively. This histogram is the rotation of X by $-10°$, Y by $150°$, Z by $-10°$ at the origin. We found that the three-dimensional histogram in this case shows some identifiable clusters.

The fog information was obtained by using a combination of channels and applying it to a third. When the information of fog is inserted into each channel, the corresponding cluster turns from gray to yellow. In Fig. 4(a), the results of a three-dimensional analysis are superimposed on the picture obtained from CH1, in yellow. As the result of image processing, it becomes apparent that this area corresponds to fog.

If the fog's cluster is displayed in the three-dimensional histogram, the three-dimensional analysis can be regarded

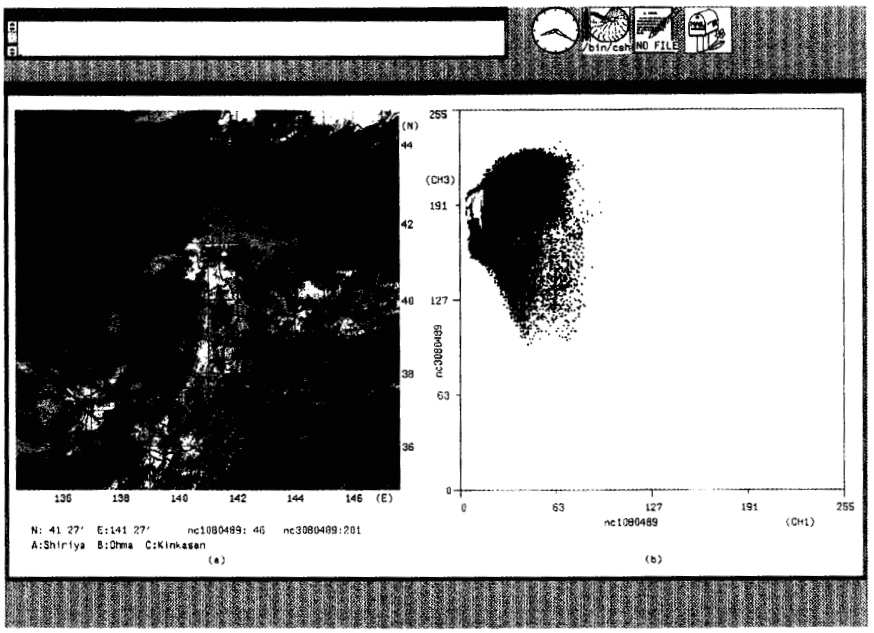

(a) (b)

Fig. 3. (a) Object area in CH1, and (b) a two-dimensional histogram of CH1 and CH3.

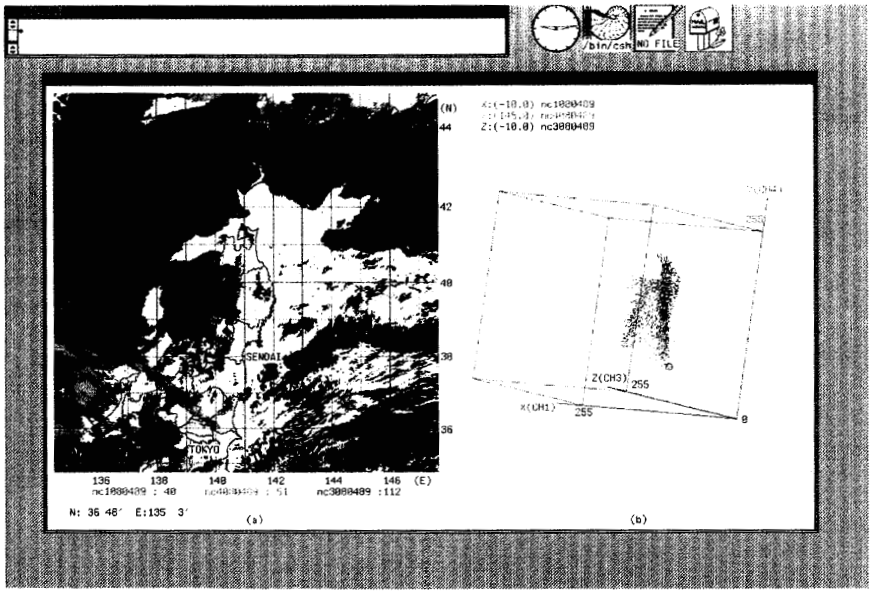

(a) (b)

Fig. 4. (a) Results of the fog analysis using the three-dimensional analysis of CH1, CH3, and CH4 and (b) the three-dimensional histogram.

as a means to find the ranges of X, Y, and Z of the cluster. We found the simplest method to be that of detecting the ranges directly from the three-dimensional histogram. This method needs free rotation of the three axes and displays the control process in real time. In that case, the computer simply requires 360^3 patterns and 256^3 memory size.

In this study, we developed the special method in which the cluster was detected from projection on $X - Y$, $Y - Z$, and $Z - X$ planes. This method can decide the ranges

of X, Y, and Z axes of the cluster by using $2 \times$ two-dimensional analyses of different combinations. It requires only 2×256^2 memory size, if the three axes are kept fixed.

The fog information was obtained by using a combination of channels and applying it to a third. In Fig. 4(a), the results of a three-dimensional analysis is superimposed, on the picture obtained from CH1, in yellow color. As the result of image processing, it seems that this area corresponds to fog.

Also we found that the results show the existence of cloud that is not fog, i.e., we are able to distinguish between fog and cloud. In addition, we found that cloud was over the fog in the western area of the analysis. An arrow pointing to the area around N: 37°, E: 135° is marked as a circle on the three-dimensional histogram in Fig. 4(b), in which the cluster was different from the yellow one differentiating cloud from fog.

The fog areas from Table I were included in all analyses, and these results correspond to a meteorologist's observations. In this way, three-dimensional analysis is shown to be a powerful tool to identify the fog.

V. Discussion

Fig. 3 shows the results in which fog was correlated to image information from CH3 and CH1. The brightness level of CH3 (nc3080489) cross-marked in Fig. 3(a) is 201. In Fig. 4(a), the brightness temperature level of the arrow pointed area (around N: 37°, E: 135°), from CH3 is 112. It is difficult to figure out the difference between fog and cloud strictly, but we have tried to classify them roughly. The reason that the brightness temperature of fog is higher than that of cloud in CH3 is as follows:

(1) The wavelength band of CH3 is near 4 μm, which belongs to both an emitted thermal band and a reflected solar band [11]. The emissivity of fog is generally lower than that of cloud and the reflectivity of fog is higher than that of cloud [12]. Even if the emissivity is the same, the reflectivity of fog is higher. In Fig. 2(a), whiter areas are considered higher reflectivity regions.

(2) In general, the height of fog is lower than that of cloud. So, usually the temperature of fog is higher than cloud in daytime CH3 imagery, resulting in higher brightness temperature of fog than of cloud.

In Fig. 4(b), the yellow cluster, which represents fog, in the three-dimensional histogram is on the upper side on the Y-axis (CH4 temperature), whereas the circle representing cloud is on the lower side. Thus the three-dimensional histogram supports this second reason cited in the last paragraph.

We found that, even as early as 0706 local, the brightness temperature of CH3 (112) is significantly higher than CH4 (51) (Fig. 4(b)). This is because of both emitted thermal and reflected solar contributions at CH3 wavelengths. It is difficult for nonmeteorologists to identify the features of images using only CH3. Nonmeteorologists can quickly correlate the cluster in the three-dimensional histograms rather than the two-dimensional histogram to identify the regions of fog.

In Fig. 4(a), it seems that the fog area (yellow region) is too large, when compared with Fig. 3(a). Probably, a meteorologist with experience in interpreting visible and infrared satellite images could produce a more accurate analysis of fog areas, though it might take a longer time. But for a nonmeteorologist using this technique, the analysis could be a preliminary guess of fog areas for use by a marine weather forecaster of fog. In addition, analysis time from data reading to display the three-dimensional histogram takes less than 2 min using an engineering work station. We were able to develop a user-friendly three-dimensional analysis system at our lab.

The measured data from satellite are changed by conditions, such as height of satellite, height of sun, etc. So, the specific threshold values of fog's brightness cannot be fixed. In this study, a cluster (whether it is a fog or not) is identified by user. To determine the exact area of the cluster is one of the aims of this method. Though the result is a rough estimate, the three-dimensional analysis distinguishes between fog and clouds clearly.

VI. Conclusions

We have first correlated observed fog to NOAA AVHRR images by using two- and three-dimensional image analysis techniques. The conclusions of this study are as follows:

(1) Here the image of fog is analyzed in a partially objective, partially subjective way. It means that the surface observations of fog cannot be precisely extended throughout the entire extent of the fog as viewed in the satellite imagery.

(2) The fog detection has been performed in the original imagery, and the corresponding cluster feature in the three-dimensional histogram is appropriately identified.

(3) The characteristics of said cluster will be similar to fog clusters in other three-dimensional histograms, allowing for the recognition of such features as indicative of the presence of fog in the original imagery.

Acknowledgment

A debt of gratitude is extended to Prof. H. Kawamura (Tohoku University) and H. Ogawa, who provided the NOAA image data and significant discussion, and to Y. Seto and T. Bando (Second Regiona Maritime Safety Agency Headquarters), who provided the fog information. Also we would like to acknowledge Fuji Xerox Co. Ltd., which provided an engineering work station.

References

[1] J. C. Barnes and M. D. Smallwood, "TIROS-N/NOAA Series Direct Readout Services Users Guide," U.S. Department of Commerce of NOAA (1982).

[2] R. Huschke, *Glossary of Meteorology*. Boston: American Meteorology Society, 1959.

[3] H. Kaminaga, J. Kudoh, S. Noguchi, "A support system for analyz-

ing NOAA images," Papers Annual Meet, The Inst. Electroncs. Inf. & Comm. Eng. Japan, D-535, pp. 7-287, 1990.
[4] J. Kudoh and S. Noguchi, "The proposal for semi-optimum value of three dimensional histogram by using NOAA AVHRR images," *Proc. 41th Annual Conventions ISP Japan*, 3M-3, 1990.
[5] L. Lauritson, G. J. Nelson, and F. W. Porto, "Data extraction and calibration of TIROS-N/NOAA radiometers," NOAA Tech. Memo. NESS1077, 1979.
[6] M. Takagi, "Receiving system for meteorological satellite (NOAA)," *Soc. Airborne & Satellite Physical & Fishery Oceanography*, no. 6, pp. 51-63, 1983.
[7] K. Akaeda and T. Takeda, "The utilization of NOAA 7 AVHRR Channel 3 data to infer the cloud structure," *J. Inst. Weather. Japan*, vol. 30, no. 1, pp. 53-58, 1984.
[8] C. E. Livingstone, K. P. Singh, A. L. Gray, "Seasonal and regional variations of active/passive microwave signatures of sea ice," *IEEE Trans. Geosci. Remote Sensing*, vol. GE-25, no. 2, pp. 159-173, March 1987.
[9] J. Kudoh, Y. Sasaki, and K. Yoshino, "Image analysis system of x-ray micro analyzer," *J. Inst. Image Electron. Eng. Japan*, vol. 18, no. 5, pp. 313-318, 1989.
[10] J. Kudoh, S. Noguchi, A. Tsuchiyama, and M. Kitamura, "Automatic classification method for multiple images," *Proc. 40th Annual Conventions ISP Japan*, 5E-2, pp. 374-375, 1990.
[11] Y. Itakura and S. Tsutsumi, "New infrared detection system with cross-correlation method," *Trans. Inst. Electron. & Comm. Eng. Japan*, Part B, vol. 58, no. 1, pp. 8-15, 1975.
[12] H. L. Hackforth, *Infrared Radiation*. New York: McGraw-Hill Company, 1960.
[13] J. Kudoh and S. Noguchi, "A study on three-dimensional histogram of the NOAA AVHRR images," *IEEE Trans. Geosci. Remote Sensing*, vol. 29, pp. 735-740, Sept. 1991.
[14] P. M. B. Walker, CBE FRSE, *Chambers Science and Technology Dictionary*. W & R Chambers and Cambridge University Press, Cambridge, England: 1988.

Jun-ichi Kudoh, born in Akita, Japan, on December 28, 1955. He received the B.E. and M.E. degrees in metallurgy from Mining College of Akita University, and the D.E. degree in metallurgy from Tohoku University, Sendai.

He joined the Research Institute of Mineral Dressing and Metallurgy at Tohoku University in 1985. Since 1991, he has been with Computer Center Tohoku University. His main area of interest is multi-dimensional image analysis.

Shoichi Noguchi, born in Tokyo on March 5, 1930, received the B.E., M.E., and D.E. degrees in electrical communication engineering from Tohoku University, Sendai.

He joined the Research Institute of Electrical Communication at Tohoku University in 1960 and has been a professor there since 1971. Dr. Noguchi had been director of the Computer Center, Tohoku University from 1984 to 1990 and currently Director of the Research Center for Applied Information Science, Tohoku University. He was vice president of IPSJ (Information Processing Society of Japan) until June 1990. His main area of interests is theoretical information science and computer network fundamentals. He has also been active in the area of parallel processing, computer network architecture, and knowledge engineering fundamentals.